X. Zianni

X. Zianni

Dept. of Aircraft Technology, Technological Educational Institution of Sterea Ellada, 34400 Psachna, Greece
Dept. of Microelectronics, Institute for Nanoscience and Nanotechnology (INN), NCSR 'Demokritos' 15310 Athens, Greece

MODELING THE THERMOELECTRIC PROPERTIES OF MODULATED NANOCOMPOSITES

Nanocomposite materials are promising for improved thermoelectric (TE) properties compared to the constituent bulk-like materials. Main effects on electrons and phonons transport properties originate from scattering on boundaries/interfaces and energy barriers. In nanostructures with a 1D doping concentration modulation, a TE power factor enhancement was predicted in the presence of two phases for the electron transport and non-uniform thermal conductivity. We have explored the influence of the composite nanostructure dimensionality on the TE efficiency enhancement. The two- and three-dimensional non-uniform nanostructures have been modeled by a network model. Our results indicate two regimes depending on the distribution of the non-uniformity in the nanostructures. The transport properties can be interpreted by either average properties or by the formation of percolation paths for conduction. Our study indicates that a network analysis could be useful in designing thermoelectric composite materials and to interpret experimental data.

Key words: modeling; thermoelectric transport properties; nanocomposites; network analysis

Introduction

Efficient thermoelectric materials require good electron transport properties and poor thermal conductivity. Nanocomposite materials are promising materials for enhancement of the thermoelectric efficiency. In nanocomposites, the electron and phonon properties are decoupled due to the structural and/or compositional non-uniformity. So far most high performance TE units are based on inorganics/metalloids or their composites [1]. Since the discovery of TE properties of intrinsically conducting polymers such as polyanilines, polypyrroles, polythiophenes or their derivatives are intensively investigated because they possess relatively low thermal conductivity, good electrical conductivity and are easy to prepare, air stable, light weight and much less costly in their production compared to their inorganic counterparts [2, 3]. Recently, it has been demonstrated that the introduction of low dimensional nanostructures in organic composites materials [4-5] has significantly improved TE characteristics due to inter-component junctions, thereby leading to phonon scattering and hoping of charge carriers [6, 7]. In addition, the use of organic/inorganic nanocomposites has attracted much attention due their exceptional electrical, thermal and mechanical characteristics [8-16].

We have previously explored the prospects for thermoelectric (TE) efficiency enhancement in non-uniform nanostructures above the quantum confinement regime [17-18]. In this regime, electrons and phonons can be treated as bulk-like carriers experiencing effects of the non-uniformity as they move through the nanostructure. Main effects on their transport properties originate from scattering on boundaries/interfaces and energy barriers. In one-dimensional modulated nanostructures (nanowires), a TE power factor enhancement was predicted in the presence of two phases for the electron transport and non-

uniform thermal conductivity [18]. We have explored the influence of the nanostructure dimensionality on the TE efficiency enhancement. The two- and three- dimensional non-uniform nanostructures have been modeled by a network model [19]. The model is described in section II. In section III, we present the structures that we have investigated and our results on the calculated transport properties. The main conclusions are drawn in section IV.

Model

We have used a network model software for calculating the thermoelectric properties, i.e. total electric and thermal resistances and total Seebeck coefficient, of modulated composite materials [19]. The real structure of the composite sample is translated into a pixel grid where local transport properties are assigned to each pixel including bulk-like properties as well as interface properties to adjacent pixels which can be adjusted to account for real interfaces. The resulting networks are embedded between a left and a right contact, each at constant temperature and constant electrostatic potential. By using nodal analysis, the total thermal and electric resistances of the structure, as well as local voltages or temperature differences between the pixels are obtained. In an additional step, the local temperature differences are used to simulate local Seebeck voltages as voltage sources between the pixels in order to obtain the total Seebeck voltage and, thus, the Seebeck coefficient, of the structure.

Results and discussion

We have modeled nanocomposite materials consisting of two phases: the TE-phase dispersed within the M-phase. The M-phase consists of a matrix material with the properties of the bulk material. The TE-phase consists of a material with enhanced Seebeck coefficient. Concerning the conductivity, we consider that the TE-phase is dispersed in (i) a conductive M-phase or in (ii) an insulating M-phase. In the former (latter) case, the conductivity of the TE-phase is lower (higher) that the conductivity of the M-phase.

We explore the dependence of the transport properties on the composition of the nanocomposite as expressed by the percentage (%) of the bulk-like phase (M-phase) in the composite material. In Fig. 1, there are shown three schematics of the nanocomposite material with different % of the bulk-like phase.

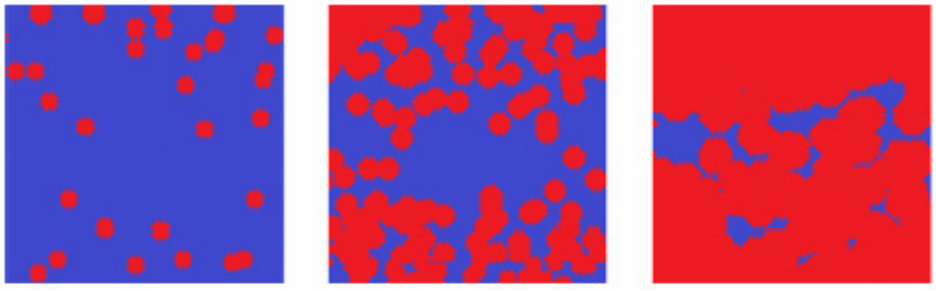

Fig. 1. A two-phase nanocomposite with the increasing ratio of the TE-phase (red) over the M-phase (blue) from left to right.

(i) TE- phase dispersed in a conductive M-phase

The transport properties of the composite material are shown in Fig. 2 and Fig.3 with respect to the transport properties of the bulk-like M-phase. In the left panel of Fig. 2, it is shown the conductivity of the nanocomposite material. The conductivity increases when the percentage of the more conductive M-phase increases. We have considered the following cases for the transport properties of the two constituent phases:

(a) uniform Seebeck coefficient and thermal conductivity (blue squares), (b) enhanced Seebeck in the TE-phase and uniform thermal conductivity (green dots), (c) enhanced Seebeck and slightly lower thermal conductivity in the TE-phase, κ_{TE}=0.8 κ_M (magenta triangles) and (d) enhanced Seebeck and strongly lower thermal conductivity in the TE-phase, κ_{TE} =0.1 κ_M (red diamonds). The conductivity of the composite material has been found the same in all cases (a)-(d). In all these cases, it increases from the TE-phase conductivity to the M-phase conductivity with increasing % of the M-phase. In the right panel of Fig. 2, it is shown that the thermal conductivity of the composite material also increases from the TE-phase thermal conductivity to the M-phase thermal conductivity with increasing % of the M-phase.

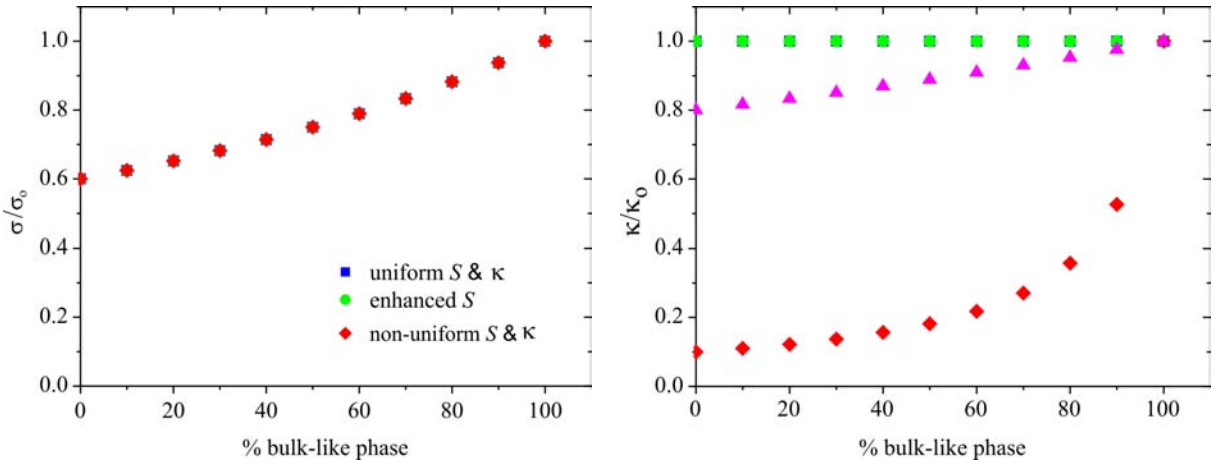

Fig. 2. The conductivity (left panel) and the thermal conductivity (right panel) of the composite material as function of the percentage of the bulk-like phase (M-phase). The symbols are explained in the main text.

The Seebeck coefficient of the composite material is shown in the left panel of Fig. 3. When the thermal conductivity of the TE-phase is the same (green dots) or slightly lower (magenta triangles) than the thermal conductivity of the M-phase, the Seebeck coefficient of the composite decreases nearly linearly with increasing % of the M-phase. A less steep decrease is found when the TE-phase has considerably lower thermal conductivity (red diamonds). In this case the composite material has enhanced Seebeck coefficient even at low concentrations of the TE-phase. In the right panel of Fig. 3, it is shown that in this case the TE power factor of the composite material is significantly enhanced. The effective TE power factor is ~4 times higher than that of the bulk-like material when a ~ 10% of the TE phase is dispersed in the composite material.

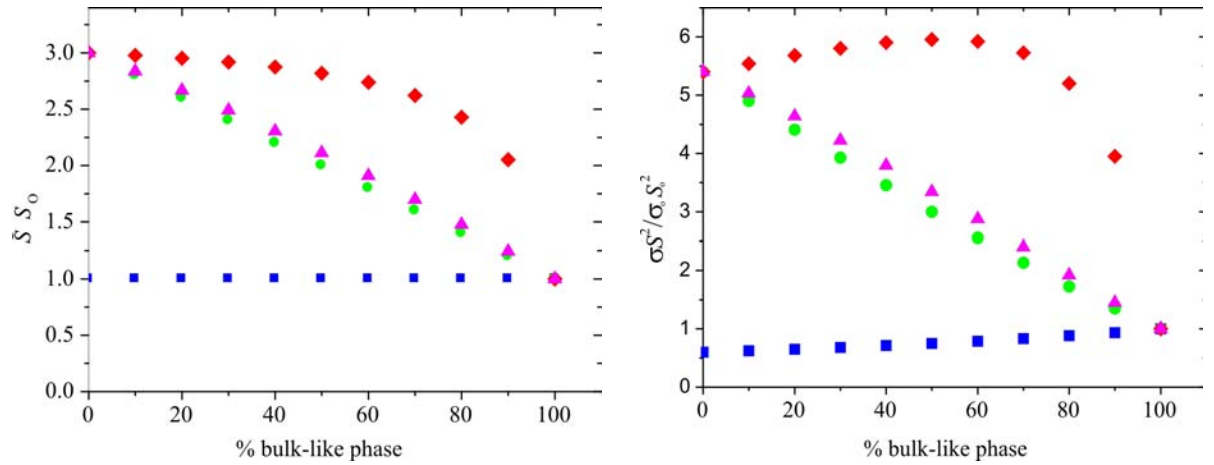

Fig. 3. The Seebeck coefficient (left panel) and the power factor (right panel) of the composite material as function of the percentage of the bulk-like phase (M-phase). The symbols are as in Fig. 2 and are explained in the main text.

(ii) TE-phase dispersed in an insulating M-phase

It has been assumed hat $\sigma_{TE} = 60\ \sigma_M$ and uniform thermal conductivity. The transport properties of the composite material are shown in Fig. 4 and 5 with respect to the transport properties of the TE-phase. The conductivity of the composite material is shown in Fig. 4 for 3D (blue diamonds), 2D (green dots), and 1D (red squares) structures. As expected, the effective conductivity decreases with increasing percentage of the M-phase. It can be noticed that the decrease is steep and shows a percolation threshold that depends on the dimensionality of the material structure. In 3D, a percolation path is formed at a rate concentration of ~.20-0.30. In 2D, a percolation path is found at ~0.5. In 1D, there is no percolation threshold because a percolation path cannot be formed. In this case, the conductivity is interpreted by the effective conductivity of a 1D in-series resistor network. The conductivity decreases smoothly with increasing percentage of the insulating M-phase.

The Seebeck coefficient is shown in the left panel of Fig. 5. The same percolation threshold behavior is found for the Seebeck coefficient as for the conductivity in 2D and 3D. A linear increase is found in the case of 1D similarly as that found for a conductive M-phase. The transport properties are interpreted in both cases (i) and (ii) by the properties of an effective medium rather by those of a percolation path.

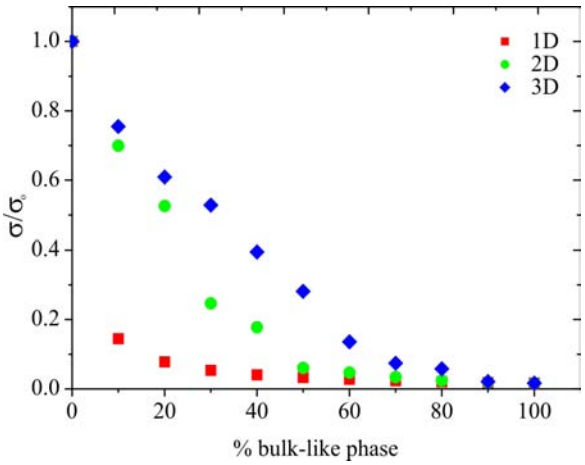

Fig. 4. The conductivity of the composite material with respect to the TE-phase conductivity for 1D (red squares), 2D (green dots) and 3D (blue diamonds) structures.

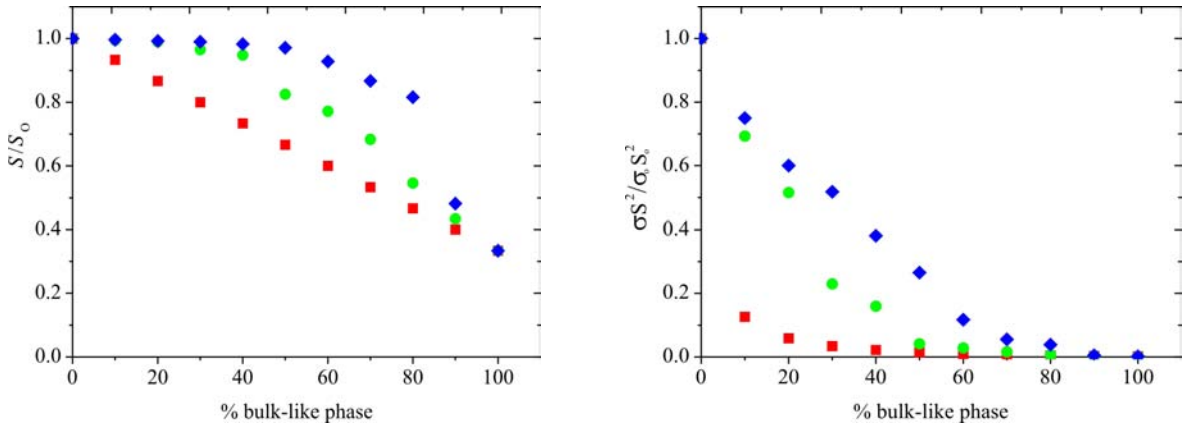

Fig. 5. The Seebeck coefficient (left panel) and the TE power factor (right panel) of the composite material with respect to the corresponding TE-phase properties for 1D (red squares), 2D (green dots) and 3D (blue diamonds) structures.

The TE power factor is shown in the right panel of Fig. 5. A very low TE power factor is found below the percolation threshold in 3D and 2D. The TE power factor increases rapidly above the

percolation threshold and is determined by the transport properties of the percolation path (TE-phase properties). In 1D, the decrease of the TE power factor is interpreted by the transport properties of the effective medium.

Conclusion

We have investigated the thermoelectric transport properties of a composite material in the presence of two phases. A bulk-like phase (M-phase) and a phase with enhanced TE properties (TE-phase). We have used a network analysis model to calculate the thermoelectric properties of the composite material. We have found that the thermoelectric properties of the composite material are strongly dependent on the material composition. Moreover, they depend on the relative transport properties of the two phases. We have identified two distinct regimes. When the M-phase is conductive, the thermoelectric properties of the composite material can be estimated by those of the effective medium with the average composition of the two phases. When the M-phase is insulating, the thermoelectric properties of the composite material are very poor below the percolation threshold. They improve rapidly above the percolation threshold and they are determined by the properties of the percolation path. Our study indicates that a network analysis could be useful in designing thermoelectric composite materials and to interpret experimental data.

Acknowledgment Funding by the European Social Fund (ESF)-European Unions and National Resources within the framework of the Grant of Excellence “ARISTEIA” is acknowledged.

References

1. A.J.Minnich, M.S.Dresselhaus, Z.F.Ren, and G.Chen, Bulk Nanostructured Thermoelectric Materials: Current Research and Future Prospects, *Energy Environ. Sci.* **2**, 466–79 (2009).
2. O.Bubnova and X.Crispi, Towards Polymer-Based Organic Thermoelectric Generators, *Energy Environ. Sci.* **5**, 9345–62 (2012).
3. N.Dubey and M.Leclerc, Conducting Polymers: Efficient Thermoelectric Materials, *J. Polym. Sci. B* **49** 467–75(2011).
4. N.Toshima, M.Imai and S.Ichikawa, Organic–Inorganic Nanohybrids as Novel Thermoelectric Materials: Hybrids of Polyaniline and Bismuth(III) Telluride Nanoparticles, *J. Electron. Mater*. **42** , 898–902(2010).
5. C.C.Liu, F.X.Jiang, M.Y.Huang, B.Y.Lu, R.R.Yue, and J.K.Xu, Free-Standing PEDOT-PSS/Ca3Co4O9 Composite Films as Novel Thermoelectric Materials *J. Electron. Mater*. **40**, 948–52 (2011).
6. M.Zebarjadi, K.Esfarjani, M.S.Dresselhaus, Z.F.Ren, and G.Chen, Perspectives on Thermoelectrics: from Fundamentals to Device Applications, *Energy Environ. Sci*. **5**, 5147–62 (2012).
7. Y.Du, S.Z.Shen, K.Cai, and P.S.Casey, Research Progress on Polymer–Inorganic Thermoelectric Nanocomposite Materials, *Prog. Polym. Sci*. **37**, 820–41(2012).
8. C.Meng, C.Liu, and S.A.Fan, A Promising Approach to Enhanced Thermoelectric Properties Using Carbon Nanotube Networks, Adv. Mater. **22,** 535–9 (2010).
9. Q.H.Wang, D.O.Bellisario, L.W.Drahushuk, R.M.Jain, S.Kruss, M.P.Landry, S.G.Mahajan, S.F.E.Shimizu, Z.W.Ulissi, and M.S.Strano, Low Dimensional Carbon Materials for Applications in Mass and Energy Transport, *Chem. Mater*. **26**, 172–83 (2014).

10. L.Wang, X.Lu, S.Lei, and Y.Song, Graphene-Based Polyaniline Nanocomposites: Preparation, Properties and Applications, *J. Mater. Chem*. **A 2,** 4491–509(2014).
11. C.Yu, Y.S.Kim, D.Kim, and J.C.Grunlan, Thermoelectric Behavior of Segregated-Network Polymer Nanocomposites, *Nano Lett*. **8**, 4428–32 (2008).
12. J.Xiang and L.T.Drzal, Templated Growth of Polyaniline on Exfoliated Graphene Nanoplatelets (GNP) and its Thermoelectric Properties, *Polymer* **53**, 4202–10(2012).
13. B.Abad, I.Alda, P.Díaz-Chao, H.Kawakami, A.Almarza, D.Amantia, D.Gutierrez, L.Aubouy, and M.Martín-González, Improved Power Factor of Polyaniline Nanocomposites with Exfoliated Graphene Nanoplatelets (GNPs), *J. Mater.Chem*. **A 1**, 10450–7 (2013).
14. C.A.Hewitt, A.B.Kaiser, S.Roth, M.Craps, R.Czerw, and D.L.Carroll, Multilayered Carbon Nanotube/Polymer Composite Based Thermoelectric Fabrics, *Nano Lett*. **12,** 1307–10 (2012).
15. D.Kim, Y.Kim, K.Choi, J.C.Grunlan, and C.Yu, Improved Thermoelectric Behavior of Nanotube-Filled Polymer Composites with Poly(3,4-ethylenedioxythiophene) Poly (styrenesulfonate), *ACS Nano* **4,** 513–23 (2010).
16. R.Islam, Chan-Yu-King Roch, J.-F.Brun, C.Gors, A.Addad , M.Depriester, A.Hadj-Sahraoui, and F.Rousse, Transport and Thermoelectric Properties of Polyaniline/Reduced Graphene Oxide Nanocomposites, *Nanotechnology* **25**, 475705-11(2014).
17. N.Neophytou, X.Zianni, H.Kosina, S.Frabboni, B.Lorenzi, and D.Narducci, Simultaneous Increase in Electrical Conductivity and Seebeck Coefficient in Highly Boron-Doped Nanocrystalline Si, *Nanotechnology* **24** (20), 205402 (2013).
18. X.Zianni , D.Narducci, Parametric Modeling of Energy Filtering in Thermoelectric Nanocomposites, *Journal of Applied Physics* **117**, 035102 (2015).
19. F.Gather, C.Heiliger, and P.J.Klar, NeMo: A Network Model Program for Analyzing the Thermoelectric Properties of Meso and Nanostructured Composite Materials, *Progress in Solid State Chemistry* **39**, 97e107 (2011).

Submitted 10.01.2015